

Long Range Correlation in Higgs Boson Plus Two Jets Production at the LHC

Peng Sun,¹ C.-P. Yuan,² and Feng Yuan¹

¹*Nuclear Science Division, Lawrence Berkeley
National Laboratory, Berkeley, CA 94720, USA*

²*Department of Physics and Astronomy,
Michigan State University, East Lansing, MI 48824, USA*

Abstract

We study Higgs boson plus two high energy jets production at the LHC in the kinematics where the two jets are well separated in rapidity. The partonic processes are dominated by the t -channel weak boson fusion (WBF) and gluon fusion (GF) contributions. We derive the associated QCD resummation formalism for the correlation analysis where the total transverse momentum q_\perp of the Higgs boson and two jets is small. Because of different color structures, the resummation results lead to distinguished behaviors: the WBF contribution peaks at relative low q_\perp while all GF channel contributions are strongly de-correlated and spread to a much wider q_\perp range. By applying a kinematic cut on q_\perp , one can effectively increase the WBF signal to the GF background by a significant factor. This greatly strengthens the ability to investigate the WBF channel in Higgs boson production and study the couplings of Higgs to electroweak bosons.

Introduction. One of the most important physics tasks after the discovery of the Standard Model (SM) Higgs boson at the CERN LHC [1, 2] is to investigate the coupling between the Higgs boson and the SM particles, in particular, the electroweak bosons. An important channel to study this coupling is through the Higgs boson plus two jets production with large rapidity separation between the jets, where the weak-boson fusion (WBF) contribution dominates over the gluon fusion (GF) contribution [3–11]. It has been further argued that because of colorless exchange in the WBF contribution as compared to color exchange in the GF contribution, they can be discriminated by the correlation study between the Higgs boson and the two jets. By imposing additional kinematic requirements to reflect the above feature will help to enhance the WBF signal to the GF background ratio. In this paper, we will demonstrate that the total transverse momentum of the Higgs boson and the two jets can be used as an important probe to distinguish the WBF and GF mechanisms.

Higgs boson plus two jets are produced in pp collisions at the LHC through

$$A(P) + B(\bar{P}) \rightarrow H + Jet_1 + Jet_2 + X , \quad (1)$$

where the incoming nucleons carry momenta P and \bar{P} , and the final state Higgs boson and the two jets with momenta P_h , k_1 and k_2 , respectively. We are interested in the kinematics that one jet is produced in the forward direction and another jet in the backward direction, while the Higgs boson in the central region. Because of the large rapidity difference between the two final state jets, i.e., $\Delta y_{12} = |y_{j1} - y_{j2}| \gg 0$, the above process is dominated by the t -channel weak boson or gluon exchange diagrams for WBF or GF contributions, respectively. In the correlation kinematics, the total transverse momentum $\vec{q}_\perp = \vec{P}_{h\perp} + \vec{k}_{1\perp} + \vec{k}_{2\perp}$ is small. The leading order diagrams $a(p_1) + b(p_2) \rightarrow c(k_1) + H(P_h) + d(k_2)$ contribute to a Delta function of $\delta^{(2)}(q_\perp)$. Due to different color structures, the WBF and GF channels will lead to different q_\perp distributions from higher order corrections. This will provide additional handle to differentiate the WBF and GF contributions in Higgs boson plus two jets production. However, the fixed order perturbative corrections lead to a singular distribution at low q_\perp . Therefore, in order to consolidate the powerful reach of the correlation study, we need to include an all order resummation. The goal of this paper is to derive the associated QCD resummation formalism and to demonstrate the powerful probe discussed above.

The QCD resummation in the low q_\perp region is referred as the transverse momentum dependent (TMD) resummation or the Collins-Soper-Sterman (CSS) resummation [12]. In our study, we follow the CSS procedure and apply recent developments on the TMD resummation for jet production in the final state [13–16]. An important feature of our derivation is the special kinematics mentioned above with $\Delta y_{12} \gg 0$ where the final state radiation associated with the jets can be resummed through a simple soft factor. The final resummation formula can be summarized into the following form, up to next-to-leading logarithmic (NLL) order,

$$\frac{d^4\sigma}{dy_h dy_{j1} dy_{j2} dk_{1\perp}^2 dk_{2\perp}^2 dq_\perp^2} \Big|_{resum.} = \sum_{ab} \sigma_0 \int \frac{d^2\vec{b}_\perp}{(2\pi)^2} e^{-i\vec{q}_\perp \cdot \vec{b}_\perp} W_{ab \rightarrow cHd}(x_1, x_2, b_\perp) , \quad (2)$$

where σ_0 represents the normalization of the differential cross section from the leading order diagrams. An all order resummation of $W(b_\perp)$ is written as

$$W(x_1, x_2, b_\perp) = \mathcal{H}(\hat{\mu}) x_1 f_a(x_1, \mu_b) x_2 f_b(x_2, \mu_b) e^{-S_a(\hat{\mu}, b_\perp) - S_b(\hat{\mu}, b_\perp)} , \quad (3)$$

where H represents the hard coefficients depending on factorization scale $\hat{\mu}$, $\mu_b = b_0/b_\perp$ with $b_0 = 2e^{-\gamma_E}$, $f_{a,b}(x, \mu_b)$ are parton distributions for the incoming partons a and b , and $x_{1,2}$

are momentum fractions of the incoming hadrons carried by the partons. (γ_E is the Euler's constant.) The two Sudakov form factors collect contributions from soft gluon radiations involved in both the initial and final states of a given partonic process, specified by the two incoming partons (a and b) of the colliding nucleons. For the parton “ a ”, we have

$$S_a(\hat{\mu}, b_\perp) = \int_{\mu_b^2}^{\hat{\mu}^2} \frac{d\mu^2}{\mu^2} \left[\ln \left(\frac{s}{\mu^2} \right) A_a + B_a + D_a \ln \frac{1}{R^2} + \gamma_a'^s \right], \quad (4)$$

where $s = (p_1 + p_2)^2$ is the total partonic center of mass energy squared, R the jet size, and A , B and D are perturbative coefficients, e.g., $A = \sum A^{(i)} (\alpha_s/2\pi)^i$. A and B are the same as those for the inclusive Z boson and Higgs boson production, via quark fusion and gluon fusion processes, respectively, with $A_q^{(1)} = C_F$, $A_g^{(1)} = C_A$, $B_q^{(1)} = -\frac{3}{2}C_F$, $B_g^{(1)} = -2\beta_0 C_A$ where $\beta_0 = 11/12 - N_f/18$. Because of the soft gluon radiation contributions associated with the final state jets, we have additional coefficients $D_q^{(1)} = C_F$ and $D_g^{(1)} = C_A$ for quark and gluon jet, respectively. (In QCD, $C_F = \frac{4}{3}$, $C_A = 3$, and N_f is the number of light quark flavors at a given energy scale.) The last term is the most important term in our calculation, because it further discriminates the WBF and GF channels in the Higgs boson plus two jets production processes. We find for each incoming parton “ a ”, depending on either WBF or GF production mechanism,

$$\gamma_{qWBF}'^s = -C_F \ln \frac{u_1}{t_1}, \quad \gamma_{qGF}'^s = (C_A - C_F) \ln \frac{u_1}{t_1}, \quad \gamma_{gGF}'^s = 0, \quad (5)$$

where $t_1 = -2k_1 \cdot p_1$ and $u_1 = -2k_1 \cdot p_2$. Similar expressions hold for parton “ b ” but with $t_2 = -2k_2 \cdot p_2$ and $u_2 = -2k_2 \cdot p_1$. In the kinematics we are interested in, i.e., $\Delta y_{12} \gg 0$ and $y_1 y_2 < 0$, we have the following relations $|u_1| \gg |t_1|$ and $|u_2| \gg |t_2|$. From the above results, we can clearly see that the leading double logarithms are universal among different channels, depending on the color charge of the incoming partons. However, the sub-leading logarithms differ among the WBF and GF channels. This additional term, proportional to $C_A \ln(u_1/t_1)$, will play a significant role to differentiate the WBF from GF processes in the proposed kinematical region, with large rapidity gap of the two forward jets, due to the fact that $|u_1| \gg |t_1|$. In the following, we will briefly present the major steps to derive the above resummation formula, and detailed derivations will be presented in a separate publication.

Asymptotic behavior at low q_\perp . As shown in Fig. 1, the leading order contributions from both WBF and GF channels lead to a Delta function in q_\perp . One gluon radiation will result into a singular behavior at low q_\perp . In the WBF channel, because of colorless exchange in the t -channel, there is no interference between the gluon radiation from the upper quark line and the lower quark line. The only nontrivial part is how to deal with the jet contribution, where we need to exclude the soft gluon radiation contributing to the final state jet functions. This exclusion will naturally introduce the jet cone size dependence in the soft gluon radiation. Following the recent developments in Refs. [14–16], we find that at low q_\perp the differential cross section can be written as

$$\begin{aligned} & \frac{\alpha_s C_F}{2\pi^2} \frac{1}{q_\perp^2} \int \frac{dx'_1 dx'_2}{x'_1 x'_2} x'_1 f_q(x'_1) x'_2 f_{q'}(x'_2) [\{\delta(\xi_2 - 1) \xi_1 \mathcal{P}_{qq}(\xi_1) + (\xi_1 \leftrightarrow \xi_2)\}] \\ & + \delta(\xi_1 - 1) \delta(\xi_2 - 1) \left(2 \ln \frac{s}{q_\perp^2} + \ln \frac{t_1 t_2}{u_1 u_2} - 3 + 2 \ln \frac{1}{R^2} \right) \Big], \quad (6) \end{aligned}$$

for the WBF contribution, where \mathcal{P}_{qq} is the quark splitting kernel. To derive the jet size dependence, we have applied the narrow jet approximation and the anti- k_t algorithm [17].

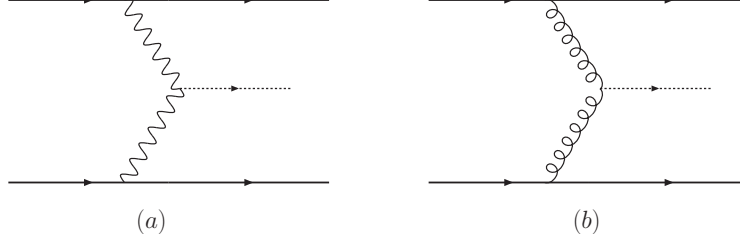


FIG. 1: Two production mechanism for Higgs plus two jets in the quark-quark scattering channel: (a) vector boson fusion and (b) gluon fusion.

However, for the GF contribution in quark-quark scattering channel, the color structure is different from the WBF contribution. In addition to the terms in Eq. (6), the interference between the quark lines gives the following additional term,

$$\frac{\alpha_s}{2\pi^2} \frac{C_A}{q_\perp^2} \ln \frac{u_1 u_2}{t_1 t_2} , \quad (7)$$

whose contribution becomes large when the rapidity difference between the two final state jets is large, namely, when $|u_1| \gg |t_1|$ or $|u_2| \gg |t_2|$. Similar results can be obtained for the gluon-gluon and quark-gluon scattering channels.

When Fourier transformed into the b_\perp space to calculate the one-loop corrections to $W(b_\perp)$, c.f. Eq. (2), the above results will contain soft divergences ($1/\epsilon^2$ in dimension regulation with $D = 4 - 2\epsilon$ dimension). These soft divergences will be canceled out by the virtual diagrams. This provides an important cross check of the above results in the low q_\perp region. The total result of real and virtual contributions will be also used to demonstrate the TMD factorization in the following section.

TMD Factorization. We follow the Collins 2011 formalism [18], where the TMD parton distributions are defined with soft factor subtraction¹. For example, the TMD quark distribution is defined as [18],

$$f_q^{sub.}(x, b_\perp, \hat{\mu}, \zeta_c) = f_q^{unsub.}(x, b_\perp) \sqrt{\frac{S^{\bar{n},v}(b_\perp)}{S^{n,\bar{n}}(b_\perp) S^{n,v}(b_\perp)}} , \quad (8)$$

where b_\perp is the Fourier conjugate variable respect to the transverse momentum k_\perp , $\hat{\mu}$ the factorization scale and $\zeta_c^2 = x^2(2v \cdot P)^2/v^2 = 2(xP^+)^2 e^{-2y_n}$ with y_n the rapidity cut-off in Collins-11 scheme. The second factor represents the soft factor subtraction with n and \bar{n} as the light-front vectors $n = (1^-, 0^+, 0_\perp)$, $\bar{n} = (0^-, 1^+, 0_\perp)$, whereas v is an off-light-front vector, and $v = (v^-, v^+, 0_\perp)$ with $v^- \gg v^+$. The un-subtracted TMD quark distribution reads as

$$f_q^{unsub.}(x, k_\perp) = \frac{1}{2} \int \frac{d\xi^- d^2\xi_\perp}{(2\pi)^3} e^{-ix\xi^- P^+ + i\vec{\xi}_\perp \cdot \vec{k}_\perp} \langle PS | \bar{\psi}(\xi) \mathcal{L}_n^\dagger(\xi) \gamma^+ \mathcal{L}_n(0) \psi(0) | PS \rangle , \quad (9)$$

with the gauge link defined as $\mathcal{L}_n(\xi) \equiv \exp\left(-ig \int_0^\infty d\lambda v \cdot A(\lambda n + \xi)\right)$. The light-cone singularity in the un-subtracted TMDs is cancelled out by the soft factor, as in Eq. (8), with

¹ Different schemes can be applied to the TMDs, which will lead to the same final resummation formula in the CSS framework [19–21].

S^{v_1, v_2} defined as

$$S^{v_1, v_2}(b_\perp) = \langle 0 | \mathcal{L}_{v_2}^\dagger(b_\perp) \mathcal{L}_{v_1}^\dagger(b_\perp) \mathcal{L}_{v_1}(0) \mathcal{L}_{v_2}(0) | 0 \rangle. \quad (10)$$

Similarly, we can define the TMD gluon distribution function.

The above TMD distribution functions (TMDs) are defined for the hard processes with color neutral particle production in the final state. To apply these TMDs in our process, we have to also include the soft gluon radiation from the final state jets. In previous studies of dijet production, the additional soft factor was expressed in the matrix form [15]. However, in the current case, the two jets are produced with large rapidity separation, and the leading contribution comes from the t -channel diagrams. Because of that, the soft factor can be simplified as

$$\begin{aligned} \mathbf{S}_{(\bar{1}, \bar{8})}(b_\perp, R; \hat{\mu}) &= \int_0^\pi \frac{d\phi_0}{\pi} \frac{C_{Iii'}^{bb'} C_{Ill'}^{aa'}}{S^{n, \bar{n}}(b_\perp)} \langle 0 | \mathcal{L}_{ncb'}^\dagger(b_\perp) \mathcal{L}_{nbc}(b_\perp) \mathcal{L}_{\bar{n}ca'}^\dagger(0) \mathcal{L}_{\bar{n}ac}(0) \\ &\quad \times \mathcal{L}_{n_1ji}^\dagger(b_\perp) \mathcal{L}_{n_2i'k}(b_\perp) \mathcal{L}_{n_2kl}^\dagger(0) \mathcal{L}_{n_1l'j}(0) | 0 \rangle, \end{aligned} \quad (11)$$

in the quark-quark scattering channel from either the color-singlet ($\bar{1}$) for the WBF contribution, or the color-octet ($\bar{8}$) for the GF contribution, respectively. To project out the color-singlet contribution we take $C_{Iii'}^{bb'} = \delta_{bb'} \delta_{ii'}$, whereas $C_{8ii'}^{bb'} = T_{bb'}^e T_{ii'}^e$ for the color-octet case. Again, we have applied the subtraction method to define the soft factor, where the light-cone singularity from the gauge links associated with the incoming partons are cancelled out. In addition, we average out the azimuthal angle ϕ_0 of the leading jet and retain the relative azimuthal angle ϕ for q_\perp , where n_1 and n_2 represent final state two quark jets' momentum directions. In deriving the soft factor $\mathbf{S}(b_\perp)$, we need to exclude soft gluon radiation contributing to the final state jet function, which falls inside the jet and leads to the jet size (R) dependence in the soft factor.

In the end, the TMD factorization for $W(b_\perp)$ can be written as

$$W(b_\perp) = f_q(x_1, b_\perp, \zeta_c; \hat{\mu}) f_q(x_2, b_\perp, \zeta_c'; \hat{\mu}) \mathbf{S}_{(\bar{1}, \bar{8})}(b_\perp; \hat{\mu}) \mathcal{H}_{TMD}(\hat{\mu}; s, t_1, u_1, t_2, u_2), \quad (12)$$

for quark-quark scattering channel from WBF ($\bar{1}$) and GF ($\bar{8}$) contributions, respectively. The TMD quark distributions are the same for both WBF and GF production mechanisms, whereas the soft and hard factors are different. The explicit calculations at one-loop order verify the above factorization formula in terms of the TMDs. We are left with the finite contributions for the hard factor \mathcal{H}_{TMD} . For WBF channel, we find that at the next-to-leading order (NLO),

$$\begin{aligned} \mathcal{H}_{TMD}^{WBF} &= 1 + \frac{\alpha_s}{2\pi} C_F \left\{ \left[\frac{1}{2} \ln^2 \left(\frac{k_{1\perp}^2}{\hat{\mu}^2} \right) - \ln \frac{k_{1\perp}^2}{\hat{\mu}^2} \left(2 \ln \frac{-t_1}{k_{1\perp}^2} + \ln \frac{1}{R^2} - \frac{3}{2} \right) - \ln^2 \left(\frac{-t_1}{k_{1\perp}^2} \right) \right. \right. \\ &\quad \left. \left. + 3 \ln \frac{-t_1}{k_{1\perp}^2} + \frac{3}{2} \ln \frac{1}{R^2} - \frac{3}{2} - \frac{5\pi^2}{6} \right] + (t_1 \leftrightarrow t_2, k_{1\perp} \leftrightarrow k_{2\perp}) \right\}, \end{aligned} \quad (13)$$

where we have taken $\zeta_c^2 = \zeta_c'^2 = s$ to simplify the final results. For the GF contribution, the hard factor is too lengthy to be listed here. We emphasize, however, that the similar logarithmic terms appear. We have also verified the TMD factorization for the gluon-gluon and quark-gluon channels, with the TMD gluon distributions from the incoming nucleons and the associated soft factors.

Resummation and Phenomenological Applications. The large logarithms are resummed by solving the relevant evolution equations for the individual factors in the TMD factorization formula in Eq. (12). For example, the TMD parton distributions obey two evolution

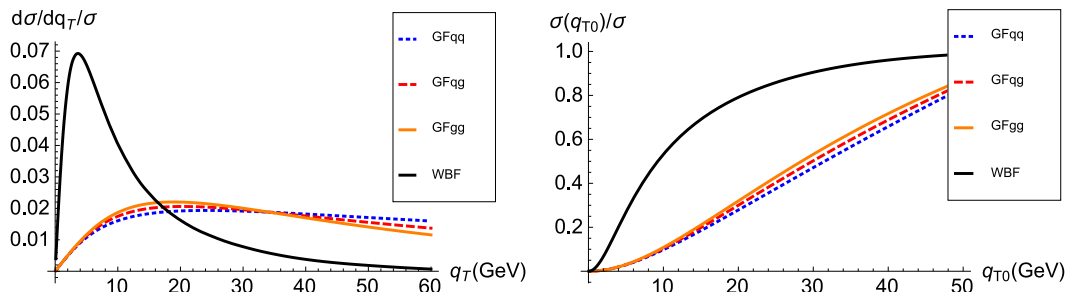


FIG. 2: Normalized distributions of the vector boson fusion and gluon-fusion contributions to the Higgs boson plus two jets production in the typical kinematics at the LHC with $\sqrt{S} = 13\text{TeV}$, where the jet transverse momenta $k_{1\perp} = k_{2\perp} = 30\text{GeV}$, $y_{j1} = -y_{j2} = 2$ and $y_h = 0$: as functions of the total transverse momentum q_\perp (left); the total rate as function of the upper limit of q_\perp (right).

equation: one is associated with the rapidity cut-off parameter ζ_c and one associated with the factorization scale $\hat{\mu}$ [18]. Additional resummation of large logarithms are carried out by solving the renormalization group equation for the soft factor, which is controlled by the associated anomalous dimension,

$$\frac{\partial}{\partial \ln \hat{\mu}} \mathbf{S}_{\bar{1},\bar{8}}(b_\perp; \hat{\mu}) = -2\gamma_{\bar{1},\bar{8}}^s \mathbf{S}_{\bar{1},\bar{8}}(b_\perp; \hat{\mu}) . \quad (14)$$

From the one-loop calculations, we find the following results for the anomalous dimension for the soft factors in all partonic channels $ab \rightarrow cHd$,

$$\gamma_{\bar{1},\bar{8}}^s = \frac{\alpha_s}{2\pi} \left[(D_a + D_b) \ln \frac{1}{R^2} + \gamma_a'^s + \gamma_b'^s \right] , \quad (15)$$

where $\gamma_{a,b}'^s$ have been given in Eq. (5) and $D_{a,b}$ defined as before. The final resummation formulas of Eqs. (2)-(5) are obtained by solving the above mentioned evolution equations. Choosing the factorization scale $\hat{\mu} \approx k_{1\perp} \sim k_{2\perp}$ will reduce the large logarithms in the hard factors.

We would like to emphasize that the resummation formulas of Eqs. (2)-(5) for the WBF contribution are also valid in all rapidity regions for the final state Higgs boson and the two jets. This is because, there are only t -channel color-less exchange diagrams contributing to the WBF process, and the relevant derivations above work for all kinematics. This is very much similar to the structure function approach for the inclusive cross section for Higgs boson production through WBF channels studied in Ref. [22].

In the following, we will apply the resummation formulas of Eqs. (2)-(5) to calculate the q_\perp distribution via either WBF or GF mechanisms, and show how to use the q_\perp distribution to enhance the WBF and suppress the GF contributions. This is important for further testing the Standard Model prediction of the couplings of Higgs boson to weak gauge bosons. For illustration purpose, we examine the case that the Higgs boson is produced in the central rapidity region with $y_h = 0$, while the two jets are in forward or backward rapidity regions with $y_{j1} = 2$ and $y_{j2} = -2$. For the numeric calculations, we use the CT10 NLO parton distribution functions [23], and take the Sudakov resummation coefficients listed in the Introduction. The non-perturbative form factors are adopted from a recent study in

Ref. [24]. We have also checked other existing parameterizations (e.g., those in Ref. [25]) and found negligible difference in the numerical results. In the left panel of Fig. 2, we plot the normalized distributions as functions of q_\perp separately in the WBF and three different GF production channels: $\frac{1}{\sigma^{tot}} \frac{d\sigma}{dq_\perp}$ with σ^{tot} obtained by integrating over q_\perp from 0 up to 60 GeV in each channel. Clearly, we find that the WBF contribution peaks around 5-7 GeV, whereas the GF contributions (via qq , qg or gg scattering processes) produce much wider q_\perp distributions. This is a direct consequence of the difference in the Sudakov form factor coefficients associated with different scattering processes, cf. Eq. (5). When the two jets are produced with large rapidity separation, we have $|u_1 u_2| \gg |t_1 t_2|$, and the difference between γ_{qGF}^s and γ_{qWBF}^s leads to a significant broadening in the q_\perp distribution for the GF contribution as compared to the WBF contribution. It is also interesting to notice that all the GF channels (via qq , qg or gg scattering processes) have similar distributions, despite the fact that the additional term γ_{gGF}^s , associated with the incoming gluon in the (qg or gg) GF processes vanishes, cf. Eq. (5). This is because A_g is proportional to C_A and the double log term dominates the Sudakov factor $S_g(\hat{\mu}, b_\perp)$ associated with the incoming gluon to result in similar q_\perp distributions in all three GF processes, as shown in Fig. 2. Physically, they all come from t -channel gluon exchange, and gluon radiation in the large rapidity interval between the two jets generate large Sudakov effects.

The dramatical difference in the q_\perp distributions of the Higgs boson plus two jet system in the WBF and GF processes provides an important tool to distinguish these two production mechanisms. To further demonstrate this point, in the right panel of Fig. 2 we plot the ratio of the integrated cross section over σ^{tot} as functions of the upper limit of the integration, denoted as $q_{\perp 0}$ there. Integrated up to 20 GeV, the WBF contribution is already at 80% of the integrated cross section up to 60 GeV, while the GF contribution only reaches to 28% of the integrated cross section of individual GF subprocess. Hence, we conclude that the predicted q_\perp distributions can be used to further discriminate the production mechanisms of the Higgs boson plus two jets with large rapidity separation. In this kinematics, the WBF and GF production processes are characterized by the exchange of a colorless weak boson or a colored gluon, respectively. Requiring an upper limit in q_\perp value will increase the fraction of the data sample induced by WBF, in contrast to GF, process. This will greatly benefit the detailed investigation of the Higgs-electroweak boson coupling from this process.

Summary and discussions. In this paper, we have derived, for the first time, the QCD resummation formula for the Higgs boson plus two jets production at the LHC, in the most interesting kinematics that the two jets are separated with large rapidity difference. Explicit one-loop calculations for both WBF and GF contributions were performed, and all order resummation formulas were obtained in the low q_\perp region of the total transverse momentum of the Higgs boson and two jets. We have also demonstrated that an additional upper limit on q_\perp will enhance the WBF signal as compared to the GF background. The low q_\perp region also corresponds to the back-to-back correlation region in the azimuthal angular distribution between the Higgs boson and the two jets. Further studies shall follow to combine our resummation formulas with the existing codes for NLO calculations, such as MCFM [26] and VBFNLO [27], to have more detailed phenomenological investigations. Theoretically, we should also pursue the QCD resummation derivation for generic kinematics of Higgs boson plus two jets production, where a matrix form will be required for the GF contributions, similar to the dijet production process. For the WBF contribution, our resummation formulas, Eqs. (2)-(5), can be applied to all the kinematic regions of Higgs boson plus two jets production in hadron collision.

From our derivations, we have shown that the GF contributions are dominated by the t -channel gluon exchange diagrams, which generate a significant resummation effects in terms of $\ln(u_1 u_2)/(t_1 t_2)$. These enhancements will increase with rapidity difference Δy_{12} between the two jets. In our calculations, we have formulated these contributions as a TMD soft factor, and resummation was carried out by following the CSS procedure. At very large rapidity separation, we may have to consider the BFKL resummation, similar to that of the so-called Mueller-Navelet dijet production [28, 29]. How and when we should include BFKL dynamics is an important question that needs further investigations.

Last, we would like to emphasize that the method developed in this paper can be applied to the new physics search as well. Especially, for the new particle production through the weak boson fusion processes, the resummation would be similar to the WBF contribution to the Higgs boson plus two jets production. Therefore, we can apply the same kinematic cut in q_\perp to enhance the new physics signal as compared to the QCD background.

This material is based upon work supported by the U.S. Department of Energy, Office of Science, Office of Nuclear Physics, under contract number DE-AC02-05CH11231, and by the U.S. National Science Foundation under Grant No. PHY-1417326.

-
- [1] G. Aad *et al.* [ATLAS Collaboration], Phys. Lett. B **716**, 1 (2012).
 - [2] S. Chatrchyan *et al.* [CMS Collaboration], Phys. Lett. B **716**, 30 (2012).
 - [3] G. Aad *et al.* [ATLAS Collaboration], arXiv:1407.4222 [hep-ex].
 - [4] G. Aad *et al.* [ATLAS Collaboration], arXiv:1408.3226 [hep-ex].
 - [5] G. Aad *et al.* [ATLAS Collaboration], arXiv:1408.7084 [hep-ex].
 - [6] J. M. Campbell, R. K. Ellis and G. Zanderighi, JHEP **0610**, 028 (2006) [hep-ph/0608194].
 - [7] J. M. Campbell, R. K. Ellis, R. Frederix, P. Nason, C. Oleari and C. Williams, JHEP **1207**, 092 (2012) [arXiv:1202.5475 [hep-ph]].
 - [8] T. Figy, C. Oleari and D. Zeppenfeld, Phys. Rev. D **68**, 073005 (2003) [hep-ph/0306109].
 - [9] see, for example, R. K. Ellis, W. T. Giele and G. Zanderighi, Phys. Rev. D **72**, 054018 (2005) [Erratum-ibid. D **74**, 079902 (2006)] [hep-ph/0506196].
 - [10] S. Gangal and F. J. Tackmann, Phys. Rev. D **87**, no. 9, 093008 (2013).
 - [11] S. Dittmaier, S. Dittmaier, C. Mariotti, G. Passarino, R. Tanaka, S. Alekhin, J. Alwall and E. A. Bagnaschi *et al.*, arXiv:1201.3084 [hep-ph]; S. Heinemeyer *et al.* [LHC Higgs Cross Section Working Group Collaboration], arXiv:1307.1347 [hep-ph].
 - [12] J. C. Collins, D. E. Soper and G. F. Sterman, Nucl. Phys. B **250**, 199 (1985).
 - [13] A. Banfi, M. Dasgupta and Y. Delenda, Phys. Lett. B **665**, 86 (2008); A. Banfi and M. Dasgupta, JHEP **0401**, 027 (2004).
 - [14] A. H. Mueller, B. -W. Xiao and F. Yuan, Phys. Rev. D **88**, 114010 (2013).
 - [15] P. Sun, C.-P. Yuan and F. Yuan, Phys. Rev. Lett. **113**, no. 23, 232001 (2014); arXiv:1506.06170 [hep-ph].
 - [16] P. Sun, C.-P. Yuan and F. Yuan, Phys. Rev. Lett. **114**, no. 20, 202001 (2015).
 - [17] B. Jager, M. Stratmann and W. Vogelsang, Phys. Rev. D **70**, 034010 (2004); A. Mukherjee and W. Vogelsang, Phys. Rev. D **86**, 094009 (2012).
 - [18] J. Collins, “Foundations of perturbative QCD,” (Cambridge monographs on particle physics, nuclear physics and cosmology. 32)
 - [19] S. Catani, D. de Florian and M. Grazzini, Nucl. Phys. B **596**, 299 (2001) [hep-ph/0008184].

- [20] X. Ji, J. P. Ma and F. Yuan, Phys. Rev. D **71**, 034005 (2005); JHEP **0507**, 020 (2005).
- [21] A. Prokudin, P. Sun and F. Yuan, Phys. Lett. B **750**, 533 (2015) doi:10.1016/j.physletb.2015.09.064 [arXiv:1505.05588 [hep-ph]].
- [22] T. Han, G. Valencia and S. Willenbrock, Phys. Rev. Lett. **69**, 3274 (1992) doi:10.1103/PhysRevLett.69.3274 [hep-ph/9206246].
- [23] J. Gao, M. Guzzi, J. Huston, H. -L. Lai, Z. Li, P. Nadolsky, J. Pumplin and D. Stump *et al.*, Phys. Rev. D **89**, 033009 (2014).
- [24] P. Sun, J. Isaacson, C.-P. Yuan and F. Yuan, arXiv:1406.3073 [hep-ph].
- [25] F. Landry, R. Brock, P. M. Nadolsky and C. P. Yuan, Phys. Rev. D **67**, 073016 (2003); Phys. Rev. D **63**, 013004 (2001); P. Sun, C. -P. Yuan and F. Yuan, Phys. Rev. D **88**, 054008 (2013).
- [26] J. M. Campbell and R. K. Ellis, Nucl. Phys. Proc. Suppl. **205-206**, 10 (2010); MCFM home page, <http://mcfm.fnal.gov>.
- [27] K. Arnold *et al.*, Comput. Phys. Commun. **180**, 1661 (2009) doi:10.1016/j.cpc.2009.03.006 [arXiv:0811.4559 [hep-ph]].
- [28] A. H. Mueller and H. Navelet, Nucl. Phys. B **282**, 727 (1987).
- [29] A. H. Mueller, L. Szymanowski, S. Wallon, B. W. Xiao and F. Yuan, JHEP **1603**, 096 (2016) doi:10.1007/JHEP03(2016)096 [arXiv:1512.07127 [hep-ph]].